ANTHROPOGENIC CONTRIBUTIONS TO THE INTENSITY OF THE 2017 UNITED STATES NORTHERN GREAT PLAINS DROUGHT

Andrew Hoell, Judith Perlwitz, Candida Dewes, Klaus Wolter, Imtiaz Rangwala, Xiao-Wei Quan, and Jon Eischeid

Anthropogenic forcing made the occurrence of observed 2017 northern Great Plains drought intensity up to 1.5 times more likely through aridification due to long-term increases in evapotranspiration over precipitation.

INTRODUCTION. Drought conditions developed rapidly during the spring and summer of 2017 over the northern Great Plains states of South Dakota, North Dakota, and Montana (Fig. 1a). On 2 May 2017, the U.S. Drought Monitor (USDM) reported no drought, with only two small areas of abnormal dryness in the central part of the region (Fig. 1b). By 1 August 2017, the USDM depicted widespread drought over all of eastern Montana and the Dakotas, highlighted by areas of extreme and exceptional drought (Fig. 1c). Deemed a "billion dollar disaster,"[1] this drought sparked widespread wildfires[2] and compromised water resources, which led to the destruction of property, livestock sell-offs, and reduced agricultural production.[3] While this region is no stranger to drought (e.g., Woodhouse and Overpeck 1998),

[1] www.ncdc.noaa.gov/billings/
[2] www.nytimes.com/2017/09/07/us/montana-wildfire-drought.html
[3] www.usda.gov/media/blog/2017/10/03/million-acres-scorched-montana-wildfires

AFFILIATIONS: Hoell—NOAA/Earth System Research Laboratory Physical Sciences Division, Boulder, Colorado; Perlwitz, Dewes, Wolter, Rangwala, Quan, and Eischeid—NOAA/Earth System Research Laboratory Physical Sciences Division and Cooperative Institute for Research in the Environmental Sciences, University of Colorado, Boulder, Colorado
CORRESPONDING AUTHOR: Andrew Hoell, andrew.hoell@noaa.gov

the last comparable event occurred as far back as 1987–89 [described in Riebsame et al. (1991)].[4] Here, we investigate anthropogenic contributions to the intensity of this drought during May–July 2017 using climate model simulations.

DATA. *Drought monitoring and estimates of observed conditions.* Expert drought assessments are from the USDM. The National Drought Mitigation Center[5] archives these USDM maps, which blend observations of the hydrology and climate with reported local impacts to produce estimates of drought severity coverage.

Estimates of observed 1-m soil moisture, precipitation, evapotranspiration, and 2-m air temperature are from the North American Land Data Assimilation System version 2 (NLDAS-2; Xia et al. 2012). We use the median of three models from NLDAS-2: Mosaic (Koster and Suarez 1994), Noah-2.8 (Xia et al. 2012), and the Variable Infiltration Capacity model (VIC-4.0.3; Wood et al. 1997).

Climate model simulations. Two 40-member ensembles of historical climate simulations are diagnosed for 1920–2016. The first ensemble, called AOGCM for atmosphere–ocean general circulation model, is carried out with the Community Earth System Model (CESM) version 1 (Kay et al. 2015), a fully coupled climate model. CESM utilizes the Community Atmosphere Model version 5 (CAM5; Neale et al. 2010) and the Community Land Surface Model version 4 (CLM4; Lawrence et al. 2011), both of which are run at an approximately 1° resolution. The second ensemble, called AGCM, is carried out with CAM5 and CLM4. While ocean and sea ice conditions are calculated

[4] www.ncdc.noaa.gov/billings/events/US/1980-2017
[5] http://droughtmonitor.unl.edu/

(a) Northern Plains Region Within the United States

(b) 2 May 2017 USDM

Intensity:

- D0 Abnormally Dry
- D1 Moderate Drought
- D2 Severe Drought
- D3 Extreme Drought
- D4 Exceptional Drought

The Drought Monitor focuses on broad-scale conditions. Local conditions may vary. See accompanying text summary for forecast statements.
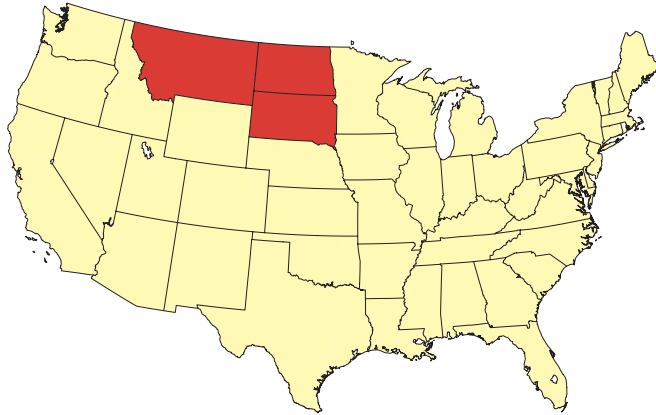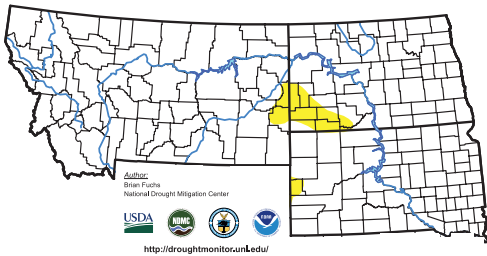
(c) 1 August 2017 USDM
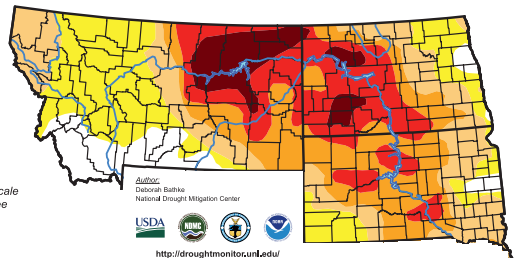
(d) July 2017 Soil Moisture

(e) May-July 2017 Precipitation

Percentile Rank Relative to 1979-2017

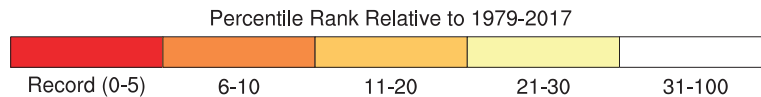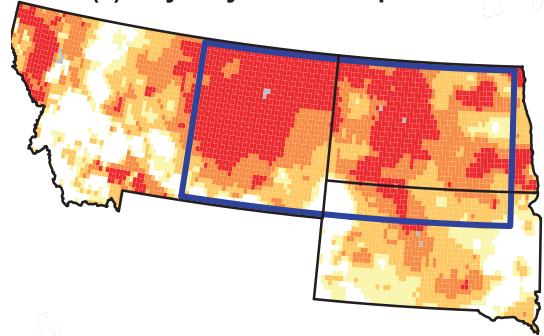| Record (0-5) | 6-10 | 11-20 | 21-30 | 31-100 |
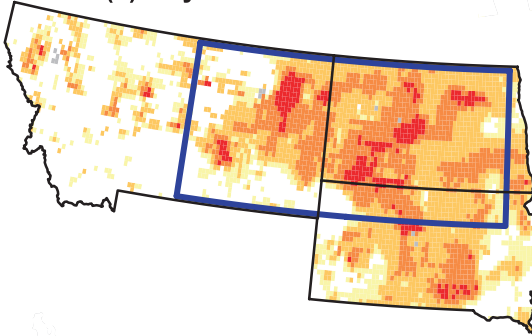
FIG. 1. (a) Location of the northern Plains. (b),(c) U.S Drought Monitor on 2 May and 1 Aug 2017, respectively. Also shown are percentile ranks of (d) July 2017 1-m soil moisture and (e) May–July 2017 precipitation based on the NLDAS-2 data. The blue box in (d) and (e) encloses the domain considered in the analysis of climate model simulations.

in AOGCM, AGCM is forced with observed time-evolving sea surface temperature and sea ice concentrations from Hurrell et al. (2008), which combines data from HadISST version 1 (Rayner et al. 2003) and NOAA OI SST version 2 (Reynolds et al. 2007). Both experiments are externally forced by the same anthropogenic (e.g., greenhouse gases and aerosols) and natural (solar and volcanic) drivers, according to the design protocol for phase 5 of the Coupled Model Intercomparison Project (CMIP5), historical forcing for 1920–2005 (Lamarque et al. 2010), and the representative concentration pathway 8.5 (RCP8.5) scenario (Meinshausen et al. 2011; Lamarque et al. 2011) thereafter.

METHODS. We compare conditions between 1920–49 and 1987–2016, referred to as the *past* and *current* climates, respectively. The comparison between past and current climates in the AOGCM and AGCM ensembles isolates the effect of changes in the prescribed external forcing, which is mostly anthropogenic (Bindoff et al. 2013). It is important to note that while the AOGCM and AGCM ensembles employ different experimental designs, they still utilize the same atmosphere and land surface models.

Our choice of past climate overlaps the "Dust Bowl" era of the 1930s. Conflicting results exists as to whether the Dust Bowl over the northern Plains was forced by sea surface temperatures (cf. Schubert et al. 2004; Hoerling et al. 2009). The choice of past climate period does not affect our results since neither experiment indicates that the severity and duration of the Dust Bowl was forced by the boundary conditions (sea surface temperatures in the case of AGCM and external forcing in the case of both AGCM and AOGCM).

We compare histograms of 1-m soil moisture, precipitation, evapotranspiration, and 2-m air temperature—and the relationships among those variables—between the simulated past and current climates over the northern Plains. The term "northern Plains" hereafter refers to areal averages over the region bounded by the blue box in Figs. 1d and 1e, the area in which soil moisture was lowest across the region during July 2017. Four classes of agricultural drought intensity are considered based on 1-m soil moisture percentile ranges (0–2, 3–5, 6–10, and 11–20), which are analogous to those considered by USDM.[6] Soil moisture thresholds associated with these percentiles are calculated relative to the past climate. The Kolmogorov–Smirnov test is used to examine whether the probability estimated from sample values between the past and current climates are of the same distribution. The change in drought risk and associated confidence intervals between past and current climates is also examined.

RESULTS. Soil moisture during July 2017 for the northern Plains region was the fifth lowest (12th percentile) between 1979 and 2017 (Fig. 1d). Widespread soil moisture in the lowest 20th percentile was observed across the region. Some areas were especially affected, as Glasgow in northeast Montana and Bismarck in central North Dakota experienced their lowest July soil moisture in 2017 since at least 1979. The

climate model experiments suggest that anthropogenic greenhouse forcing has contributed to the intensity of the drought by driving long-term reductions in soil moisture (referred to hereafter as aridification). From past to current climate, the simulations exhibit significant ($p < 0.001$) northern Plains soil moisture declines of 2%, which corresponds to 0.5 standard deviations (σ) of the past climate's interannual variability (Fig. 2a; see also Fig. ES1a in the online supplemental material). The aridification of July soil moisture is also notable in the scatter of soil moisture, as there is a clear shift to lesser values in the current climate relative to the past (Figs. 2e,f and ES2e,f).

Consistently, the aridification during July increased the risk of summertime northern Plains agricultural droughts (Table 1). Specifically, droughts in the 11th–20th soil moisture percentile, such as during July 2017, are found to occur 1.2–1.5 times more often in the current climate than in the past climate. For more intense droughts, the risk of occurrence is even more enhanced with droughts in the 3rd–5th and 0th–2nd soil moisture percentiles occurring 1.7–2 times and 3–5 times more frequently in the current climate than in the past climate, respectively.

The observed drought was largely driven by low May–July precipitation over the northern Plains (Fig. 1e). Record low precipitation since 1979 was observed over at least 50% of the northern Plains region, mainly over northeastern Montana and North Dakota. However, the climate model experiments show a slight but significant increase (at $p < 0.04$) in northern Plains precipitation (Figs. 2b and ES1b), indicating that an anthropogenically driven increase in risk of specific drought intensities is not caused by precipitation changes. Rather, the aridification of the northern Plains during July is forced by statistically significant ($p < 0.001$) increases in evapotranspiration (0.4σ; Fig. ES2c) during May–July associated with statistically significant ($p < 0.001$) increases in May–July 2-m air temperature by 0.5–0.6 K (0.5σ; Figs. 2d and ES2d). Previous studies show that many of the twentieth-century temperature changes over North America are attributable to human influences in coupled climate models (e.g., Knutson et al. 2013). Our findings are consistent with a body of literature that suggests that anthropogenic influences decreases soil moisture and increases the risk of agricultural drought over North America through increases in evaporation as a result of human-induced warming (e.g., Hoerling et al. 2008; Sheffield and Wood 2011).

May–July precipitation and July soil moisture are closely linked ($r = 0.76$; Figs. 2e,f and ES2e,f) in both past and current climates. Taking into account the
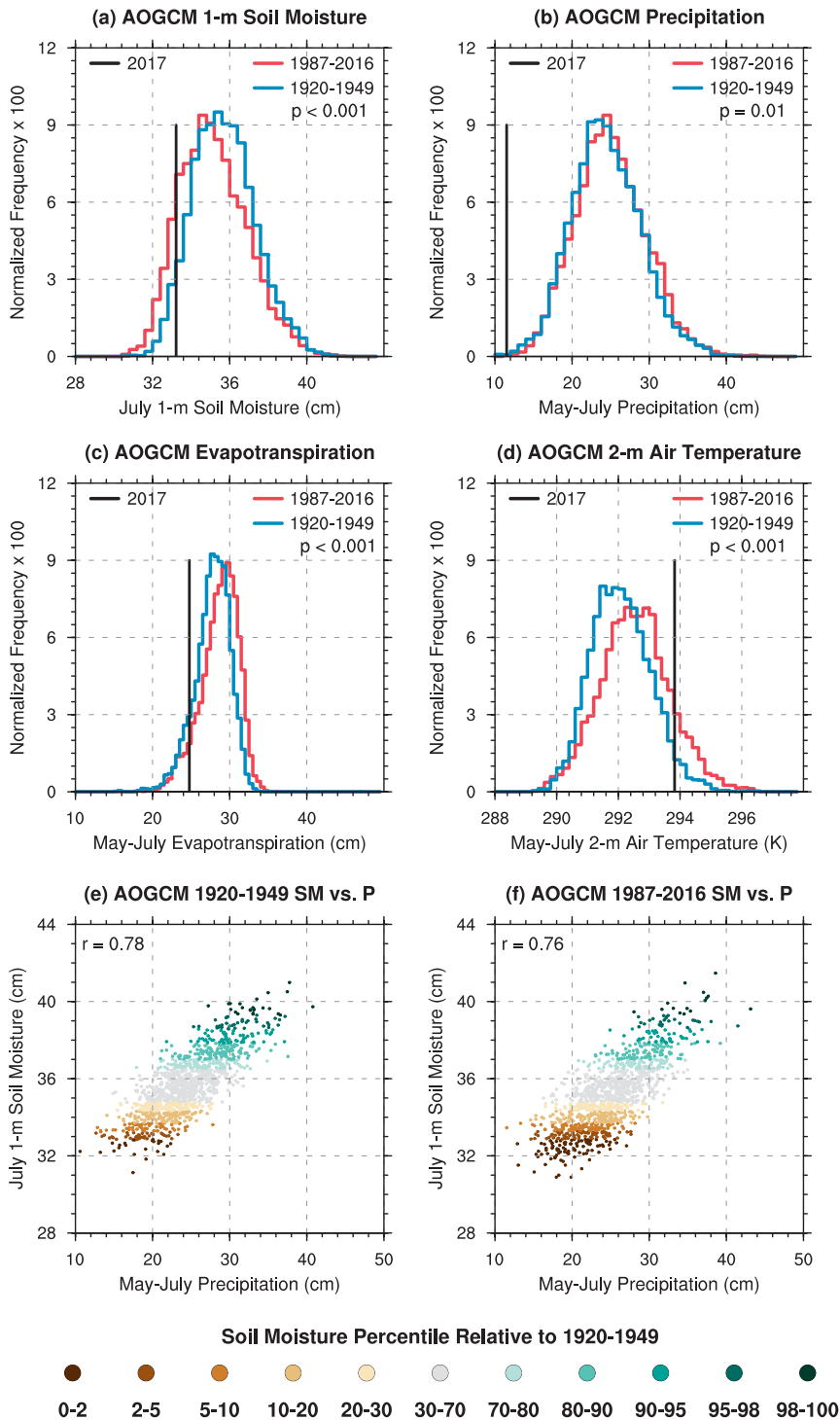
---

[6] http://droughtmonitor.unl.edu/AboutUSDM/DroughtClassification.aspx

Fig. 2. Results from AOGCM areally averaged over the northern Plains. Normalized histograms of (a) July 1-m soil moisture, (b) May–July precipitation, (c) May–July evapotranspiration, and (d) May–July 2-m air temperature (cm) for 1987–2016 (red) and 1920–49 (blue). Black line in (a)–(d) displays NLDAS-2 percentile rank for 2017 at the value corresponding to the same percentile rank in the model simulations of the current climate. Also shown are scatter diagrams of July 1-m soil moisture and May–July precipitation during (e) 1920–49 and (f) 1987–2016.

small precipitation change between past and current climates, we can illustrate, however, that specific precipitation amounts above certain percentiles are less effective at keeping the northern plain regions out of drought (see Table ES1 in the online supplemental material; shift in scatter to lower soil moisture values from past to current climate in Figs. 2e,f and ES2e,f). For example, there is up to a 3.5-fold increased risk in drought occurrence when precipitation falls in the 40th–50th percentile range. Even for lower precipitation percentiles (e.g., 2nd–10th), where it is expected that drought occurs more frequently in general, there is still a 30% increase in drought occurrence from the past to the current climate.

For May–July 2017, which was the driest since at least 1979 over the northern Plains (Fig. 1e), both the AGCM and AOGCM experiments reveal that drought during July 2017 would have likely occurred regardless of external forcing (Table ES2). We found that in both past and current climates there is a 92% chance that simulated 1-m soil moisture falls in the lower 20th percentile when May–July precipitation values are in the lower second percentile.

CONCLUSIONS. We estimated the anthropogenic contributions to the intensity of agricultural drought over the United States northern Great Plains during May–July 2017 using model simulations. The experiments

TABLE 1. Relative risk of drought intensity between current and past climates as a function of July soil moisture percentiles in AOGCM and AGCM simulations.

Soil moisture percentile	AOGCM			AGCM		
	Lower 95% CI	Risk	Upper 95% CI	Lower 95% CI	Risk	Upper 95% CI
21–30	0.8	1.0	1.3	1.0	1.2	1.5
11–20	1.0	1.2	1.5	1.3	1.5	1.9
6–10	1.1	1.5	2.0	1.3	1.8	2.4
3–5	1.4	2.0	3.0	1.27	1.7	2.6
0–2	2.2	3.4	5.4	3.4	5.2	8.0

reveal that climate change made droughts with an intensity similar to that observed in May–July 2017 up to 1.5 times more likely as a result of aridification due to increases in evapotranspiration over precipitation. However, the principal cause of the 2017 drought was record low precipitation. We found that for such record low May–July 2017 (0th–2nd percentile) precipitation, drought (as defined by soil moisture below the 20th percentile) occurs with the same frequency in the simulated current and past climates.

REFERENCES

Bindoff, N. L., and Coauthors, 2013: Detection and attribution of climate change: From global to regional. *Climate Change 2013: The Physical Science Basis*, T. F. Stocker et al, Eds., Cambridge University Press, 867–952.

Hoerling, M., G. Hegerl, D. Karoly, A. Kumar, and D. Rind, 2008: Attribution of the causes of climate variations and trends over North America during the modern reanalysis period. *Reanalysis of Historical Climate Data for Key Atmospheric Features: Implications for Attribution of Causes of Observed Change,* R. Dole, M. Hoerling, and S. Schubert, Eds., National Climatic Data Center, 47–92.

——, X.-W. Quan, and J. Eischeid, 2009: Distinct causes for two principal U.S. droughts of the 20th century. *Geophys. Res. Lett.*, **36**, L19708, https://doi .org/10.1029/2009GL039860.

Hurrell, J. W., J. J. Hack, D. Shea, J. M. Caron, and J. Rosinski, 2008: A new sea surface temperature and sea ice boundary dataset for the Community Atmosphere Model. *J. Climate*, **21**, 5145–5153, https://doi .org/10.1175/2008JCLI2292.1.

Kay, J. E., and Coauthors, 2015: The Community Earth System Model (CESM) Large Ensemble Project: A community resource for studying climate change in the presence of internal climate variability. *Bull. Amer. Meteor. Soc.*, **96**, 1333–1349, https://doi.org/10.1175 /BAMS-D-13-00255.1.

Knutson, T. R., F. Zeng, and A. T. Wittenberg, 2013: Multimodel assessment of regional surface temperature trends: CMIP3 and CMIP5 twentieth-century simulations. *J. Climate*, **26**, 8709–8743, https://doi .org/10.1175/JCLI-D-12-00567.1.

Koster, R. D., and M. J. Suarez, 1994: The components of a 'SVAT' scheme and their effects on a GCM's hydrological cycle. *Adv. Water Resour.*, **17**, 61–78, https:// doi.org/10.1016/0309-1708(94)90024-8.

Lamarque, J. F., and Coauthors, 2010: Historical (1850–2000) gridded anthropogenic and biomass burning emissions of reactive gases and aerosols: Methodology and application. *Atmos. Chem. Phys.*, **10**, 7017–7039, https://doi.org/10.5194/acp-10-7017 -2010.

——, G. P. Kyle, M. Meinshausen, K. Riahi, S. J. Smith, D. P. van Vuuren, A. J. Conley, and F. Vitt, 2011: Global and regional evolution of short-lived radiatively-active gases and aerosols in the representative concentration pathways. *Climatic Change*, **109**, 191–212, https://doi .org/10.1007/s10584-011-0155-0.

Lawrence, D. M., and Coauthors, 2011: Parameterization improvements and functional and structural advances in version 4 of the Community Land Model. *J. Adv. Model. Earth Syst.*, **3**, M03001, https://doi .org/10.1029/2011MS00045.

Meinshausen, M., and Coauthors, 2011: The RCP greenhouse gas concentrations and their extension from 1765 to 2300. *Climatic Change*, **109**, 213–241, https:// doi.org/10.1007/s10584-011-0156-z.

[7] www.drought.gov/drought/
[8] www.esrl.noaa.gov/psd/repository/alias/facts

Neale, R. B., and Coauthors, 2010: Description of the NCAR Community Atmosphere Model (CAM5.0). NCAR/TN-486+STR, 274 pp., www.cesm.ucar.edu/models/cesm1.0/cam/docs/description/cam5_desc.pdf.

Rayner, N. A., D. E. Parker, E. B. Horton, C. K. Folland, L. V. Alexander, D. P. Rowell, E. C. Kent, and A. Kaplan, 2003: Global analyses of sea surface temperature, sea ice, and night marine air temperature since the late nineteenth century. *J. Geophys. Res.*, **108**, 4407, https://doi.org/10.1029/2002JD002670.

Reynolds, R. W., T. M. Smith, C. Liu, D. B. Chelton, K. S. Casey, and M. G. Schlax, 2007: Daily high-resolution-blended analyses for sea surface temperature. *J. Climate*, **20**, 5473–5496, https://doi.org/10.1175/2007JCLI1824.1.

Riebsame, W. E., S. A. Changnon, and T. R. Karl, 1991: *Drought and Natural Resources Management in the United States: Impacts and Implications of the 1987–89 Drought.* Westview Press, 174 pp.

Schubert, S. D., M. J. Suarez, P. J. Pegion, R. D. Koster, and J. T. Bacmeister, 2004: On the cause of the 1930s Dust Bowl. *Science*, **303**, 1855–1859, https://doi.org/10.1126/science.1095048.

Sheffield, J., and E. Wood, 2011: *Drought: Past Problems and Future Scenarios.* Earthscan, 210 pp.

Wood, E. F., D. Lettenmaier, X. Liang, B. Nijssen, and S. W. Wetzel, 1997: Hydrologic modeling of continental-scale basins. *Annu. Rev. Earth Planet. Sci.*, **25**, 279–300, https://doi.org/10.1146/annurev.earth.25.1.279.

Woodhouse, C. A., and J. T. Overpeck, 1998: 2000 years of drought variability in the central United States. *Bull. Amer. Meteor. Soc.*, **79**, 2693–2714, https://doi.org/10.1175/1520-0477(1998)079<2693:YODVIT>2.0.CO;2.

Xia, Y., and Coauthors, 2012: Continental-scale water and energy flux analysis and validation for the North American Land Data Assimilation System project phase 2 (NLDAS-2): 1. Intercomparison and application of model products. *J. Geophys. Res.*, **117**, D03109, https://doi.org/10.1029/2011JD016048.